

NUMERICAL SIMULATION OF A FLOW OVER A CIRCULAR CYLINDER USING IMMERSED BOUNDARY METHOD IN VORTICITY-VELOCITY FORMULATION

Leandro F. de Souza

Instituto de Ciências Matemáticas e de Computação, Departamento de Ciências de Computação e Estatística – USP
Av. Trabalhador São-carlense, 400 - Centro Caixa Postal: 668 - CEP: 13560-970 - São Carlos - SP, Brazil
lefraso@icmc.usp.br

Abstract. *In this work a flow over a cylinder is studied by means of numerical simulation. The domain was decomposed in Cartesian grid and the cylinder is taken into account using an immersed Boundary technique. The Navier-Stokes equations are written in vorticity-velocity formulation. A high order finite difference scheme is adopted to discretize the spatial derivatives. The time integration is carried out using a fourth order Runge-Kutta method. A buffer domain is adopted in all boundaries except at the inlet. Good agreement is found between the present calculations, previous computational and experimental results for steady and time-dependent flow at low Reynolds numbers.*

Keywords: *Immersed Boundary method, Vorticity-velocity formulation, High order finite-difference.*

1. Introduction

The research area of Computational Fluid Dynamics (CFD) is increasing every day. One reason of this is the increasing in the processing and storage capacity of the computers. However the complex phenomena in this area are restricted to simple geometries. The numerical studies of flow over bodies with complex geometries, with or without movement, requires a mesh and numerical code that are capable to reproduce the physics of the flow. Normally these kind of meshes coincides with the boundaries of the body. An alternative of this is the use of approximations where the boundaries of the body does not need to coincide with the computational mesh, allowing the use of a Cartesian grid. The great challenge of this method is the use of approximations that assures accuracy and numerical efficiency.

A technique that was introduced recently is the immersed boundary method. This method was introduced by Peskin (1972). In this work, he studied a incompressible flow in a region with immersed bodies, which moved with the flow and exerted force in it. The great advantage in the method introduced is that the Navier-Stokes equations are solved in a rectangular domain. The fluid-solid interfacial effects in his work are modeled by a force added to the Navier-Stokes source term. This force is calculated with the body configuration. To link the body with the flow, since the mesh point do not need to coincide with the body points, a function is introduced, analogous to δ function.

Goldstein et al. (1993) develop a different way of calculating the force field generated by the immersed body, suggesting an iterative control with 2 constants. In this approximation one can verify that the method works like a harmonic damped oscillator, with one constant for the spring and other for the viscous damper. The main difference between their method and the method proposed by Peskin (1972), Peskin (1977) is that the method proposed by then was developed to solve problems with rigid bodies, where the method proposed by Peskin can work with elastic bodies as well.

Saiki and Biringen (1996) use the method proposed by Goldstein et al. (1993) combined with a 4th order code. Their test case is a flow over stationary or moving cylinder. According to the authors, the use of finite difference method suppressed the numerical oscillations caused by the forcing term found by Goldstein et al. (1993), that used a spectral method. The numerical simulations covered the range of Reynolds number from 25 to 400. The numerical results suggests that when the Reynolds number is high, the forcing term should be imposed at all internal points of the body, instead of only at the boundaries. Their results were compared with experimental other numerical results, showing a good agreement and eliminating the spurious oscillations found by Goldstein et al. (1993)

Mohd-Yusof (1997) and Mohd-Yusof (1998) show an immersed boundary method that allows the study of flows over complex geometries bodies using pseudo-spectral methods. One advantage is that one can join high order of accuracy, which pseudo-spectral methods has, with the study of flows over complex geometries bodies. Other advantage is that the proposed scheme does not need an ad-hoc constant to be set.

Linnick (1999) use immersed boundary method in transitional flows with the objective of delaying the transition of a laminar flow to turbulence. The vorticity-velocity formulation is used and the immersed boundary method is verified by comparing qualitatively the results obtained in flow over a square and a circular cylinder, flow over a cavity and a boundary layer flow with a rugosity at the wall.

Lai and Peskin (2000) show an immersed boundary methods with 2nd order of accuracy. The method is tested with a flow over a cylinder of circular section. The influence of the numerical viscosity in the results is analyzed, by comparing the results with the first order code (Peskin, 1972 and Peskin, 1977). A question that may arise, when one uses their method at different Reynolds number, is how the scheme performs. In other words it is important to check whether the

numerics interfere with the physics, specially for high Reynolds number flows. Their results show that with the 2nd order method the physics are more accurately resolved and it is possible to get more stable solutions.

Balaras (2003) presents an immersed boundary method applied with a Large Eddy Simulation (LES) technique. Three test cases were done and the results obtained are compared with analytical solutions and with the results obtained by other numerical simulations. The results show that the method can reproduce the physics of the studied flows efficiently.

Linnick and Fasel (2003) use a special treatment of the derivatives in the interface fluid/body in their immersed boundary method. The spatial derivatives are calculated using a 4th order compact finite difference schemes. Their results assure that the 4th order truncation error is maintained in their studied cases.

Lima e Silva et al. (2003) develop an immersed boundary method which is applied in a study of a flow over a circular cylinder. In their method the calculation of the force field is done using the Navier–Stokes equations applied in Lagrangian points and then distributed over Eulerian grid. The advantage of this method is that the force field calculation is done without the need of adjusted constants.

In the present work an immersed boundary method is used to study low Reynolds numbers flows over a cylinder of a circular section. The Navier-Stokes equations are written in vorticity-velocity formulation. The spatial derivatives are calculated by 6th order compact finite difference schemes. The time integration is carried out by a 4th order Runge-Kutta scheme. The results obtained with the simulations are compared with other numerical results in order to verify the numerical code. The present paper is divided as follows: in the next section the formulation used is given; section 3. shows details of the numerical schemes evaluated for time integration; in Section 4 the propagation of disturbances with the different time integration schemes are given; the conclusions and final comments are given in section 5.

2. Formulation

In this study, the governing equations are the incompressible, unsteady Navier-Stokes equations with constant density and viscosity. They consist of the momentum equations for the velocity components (u, v) in the streamwise direction (x) and wall normal direction (y):

$$\frac{\partial u}{\partial t} + u \frac{\partial u}{\partial x} + v \frac{\partial u}{\partial y} = -\frac{\partial p}{\partial x} + \nabla^2 u + F_x, \quad (1)$$

$$\frac{\partial v}{\partial t} + u \frac{\partial v}{\partial x} + v \frac{\partial v}{\partial y} = -\frac{\partial p}{\partial y} + \nabla^2 v + F_y, \quad (2)$$

and the continuity equation:

$$\frac{\partial u}{\partial x} + \frac{\partial v}{\partial y} = 0, \quad (3)$$

where p is the pressure and

$$\nabla^2 = \frac{1}{Re} \left(\frac{\partial^2}{\partial x^2} + \frac{\partial^2}{\partial y^2} \right). \quad (4)$$

The variables used in the above equations are non-dimensional. They are related to the dimensional variables by:

$$x = \frac{\bar{x}}{\bar{R}}, \quad y = \frac{\bar{y}}{\bar{R}}, \quad u = \frac{\bar{u}}{\bar{U}_\infty}, \quad v = \frac{\bar{v}}{\bar{U}_\infty}, \quad t = \frac{\bar{t} \bar{U}_\infty}{\bar{R}}, \quad Re = \frac{\bar{U}_\infty \bar{R}}{\bar{\nu}},$$

where Re is the Reynolds number, the terms with an over-bar are dimensional terms: \bar{R} is the radius of the cylinder, \bar{U}_∞ is the free-stream velocity and $\bar{\nu}$ is the kinematic viscosity.

The vorticity here is defined as the negative curl of velocity vector. The vorticity transport equation is obtained by the momentum equations, Eqs. (1) and (2), and can be written as:

$$\frac{\partial \omega_z}{\partial t} = -u \frac{\partial \omega_z}{\partial x} - v \frac{\partial \omega_z}{\partial y} + \nabla^2 \omega_z + \frac{\partial F_x}{\partial y} - \frac{\partial F_y}{\partial x}. \quad (5)$$

Taking the definition of the vorticity and the mass conservation equation, one can obtain a Poisson equation for v velocity component:

$$\frac{\partial^2 v}{\partial x^2} + \frac{\partial^2 v}{\partial y^2} = -\frac{\partial \omega_z}{\partial x}, \quad (6)$$

The governing equations are complemented by the specification of boundary conditions. At the inflow the velocity and vorticity components are specified based on the Blasius boundary layer solution. At the upper and lower boundaries the vorticity disturbances decay exponentially to zero. Finally, at the outflow boundary the second derivative of all dependent variables are set to zero.

3. Numerical Method

The Eqs.(3), (5) and (6) are solved numerically inside the integration domain shown schematically in Fig. 1. This domain is the same used by Lima e Silva et al. (2003) in their numerical simulations. The calculation is done on a orthogonal uniform grid, parallel to the streamwise direction. The fluid enters the computational domain at $x = x_0$ and exits at the outflow boundary $x = x_{max}$. In the regions near outflow, upper and lower boundaries a buffer domain technique (Kloker et al, 1993 and Souza et al, 2004) was implemented in order to avoid reflections at these boundaries.

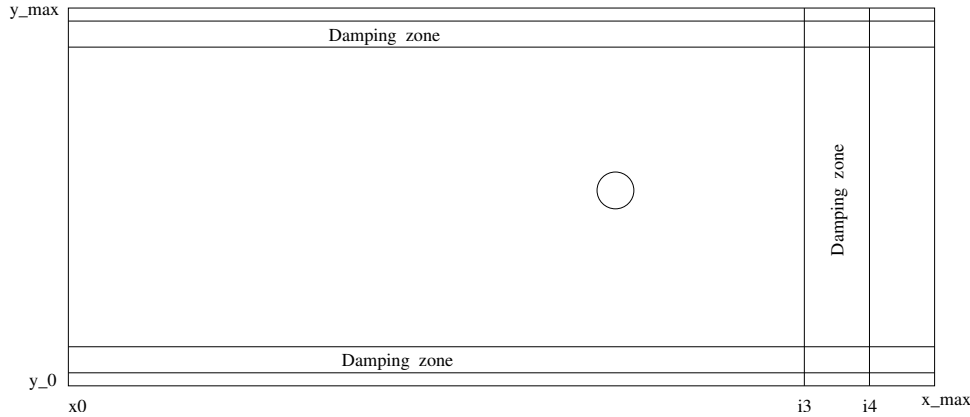


Figure 1. Integration domain.

At the inflow boundary ($x = x_0$), the velocity and vorticity components are specified. At the outflow boundary ($x = x_{max}$), the second derivative of the velocity and vorticity components in the streamwise direction are set to zero. At the upper ($y = y_{max}$) and lower ($y = 0$) boundaries, the derivatives of v in the y direction are set to zero.

Three damping zones were used in the simulations, to force the disturbances gradually damped down to zero. This technique is well documented in Kloker et al (1993), where the advantages and requirements are discussed. In the work of Meitz and Fasel (2000), a fifth order polynomial was adopted and the same function was used in the present simulations. The basic idea is to multiply the vorticity components by a ramp function $f_2(x)$ after each step of the integration scheme. This technique has prove to be very efficient in avoiding reflections that could come from the boundaries when simulating flows with disturbances. Using this technique, the vorticity components are taken as:

$$\omega_z(x, y) = f_2(x)\Omega_z(x, y, t), \quad (7)$$

where $\omega_z(x, y, t)$ is the disturbance vorticity component that comes out from the time integration scheme and $f_2(x)$ is a ramp function that goes smoothly from 1 to 0. The implemented function, in the x direction, was:

$$f_2(x) = f(\epsilon) = 1 - 6\epsilon^5 + 15\epsilon^4 - 10\epsilon^3, \quad (8)$$

where $\epsilon = (i - i_3)/(i_4 - i_3)$ for $i_3 \leq i \leq i_4$. The points i_3 and i_4 correspond to the positions x_3 and x_4 in the streamwise direction respectively. To ensure good numerical results a minimum distance between x_3 and x_4 and between x_4 and the end of the domain - x_{max} should be specified. The zones in the x direction have 30 grid points each one. Similar functions were used in the damping zones in the y direction, where 20 grid points were used in the damping zone and 10 grid points were settled between the damping zone and the boundaries.

The spatial derivatives were calculated using a 6th order compact finite difference scheme (Souza et al, 2005). The v -Poisson, Eq. (6), was solved using a Full Approximation Scheme (FAS) multigrid (Stüben and Trottenberg, 1981). A v-cycle working with 4 grids was implemented.

The boundary force values were calculated using the following equations:

$$F_x(i, j) = [F_x(i, j) + \alpha u(i, j)] \delta(i, j) \quad (9)$$

$$F_y(i, j) = [F_y(i, j) + \alpha v(i, j)] \delta(i, j), \quad (10)$$

where $\delta(i, j)$ is a value that varies from $\delta(i, j) = 0$ outside the immersed boundary to $\delta(i, j) = 1$ at the boundaries and inside the immersed boundary. The α is a negative constant used to calculate the value of the forces, and $F_x(i, j)$ and $F_y(i, j)$ are the forcing term components in x and y directions respectively. A value of $\alpha = -200.0$ was adopted, for all numerical simulations realized in the present work.

After calculating the values of F_x and F_y , their derivatives in the y and x directions, respectively, are calculated. These derivatives are used in Eq. (5). After the time integration of Eq. (5), the buffer domain technique is applied near

the outflow, lower and upper boundaries. The next step is to find the v velocity component, by solving numerically the Eq. (6); and find the u velocity by solving the Eq. (3). The "last" step is to verify the values of the velocity components inside the immersed body; if these values are below a predefined value; a next time integration step can be performed; otherwise the values of F_x and F_y have to be calculated once again and the loop described in this paragraph have to be performed. The predefined value which the velocity components are supposed to be below, adopted in the present work was 1×10^{-3} .

The numerical procedure works as described below, at each step of the Runge-Kutta scheme the following instructions are necessary:

1. Compute the spatial derivatives of the vorticity transport equation (5);
2. Calculate the immersed boundary forces F_x and F_y ;
3. Calculate the rotational of the immersed boundary force;
4. Integrate the vorticity transport equation over one step (or sub-step) of the scheme using the values obtained in steps 1 and 3;
5. Apply the buffer domain technique near the outflow, lower and upper boundaries;
6. Calculate v velocity from the v-Poisson equation (6);
7. Calculate u velocity from the continuity equation (3).
8. Verify the values of the velocity components at the immersed boundary, if they are bellow a predefined value, continue, otherwise goes to step 2;

This scheme is repeated until a stable or periodic solution is reached.

4. Numerical Results

In the simulations studied here small Reynolds numbers were adopted in order to obtain physical solutions that could be represented by a 2D simulation. Therefore 5 different Reynolds numbers were tested: 30, 45, 100, 150 and 300. The integration domain used for all tests is shown in Fig. 1. It extends from $x_0 = 0.00$ to $x_{max} = 30.00$ in the streamwise direction and from $y_0 = 0.00$ to $y_{max} = 15.00$ in the wall normal direction. The number of points used was 513 and 257 in x and y direction respectively. The distance between two consecutive points in both directions was 0.0586. The time step adopted in the simulations was 0.00785 that gives a CFL number of 0.134. The cylinder with radius of 0.5 was introduced by immersed boundary technique with its center located at $x = 16.5$ and $y = 7.5$.

At low Reynolds numbers, ($4.5 \leq Re \leq 35$), experiments reveal an attached, steady, symmetric, recirculation bubble which develops downstream of the cylinder (Saiki and Biringen, 1996) Figure 2 shows the streamlines of the flow over a cylinder with $Re = 30$.

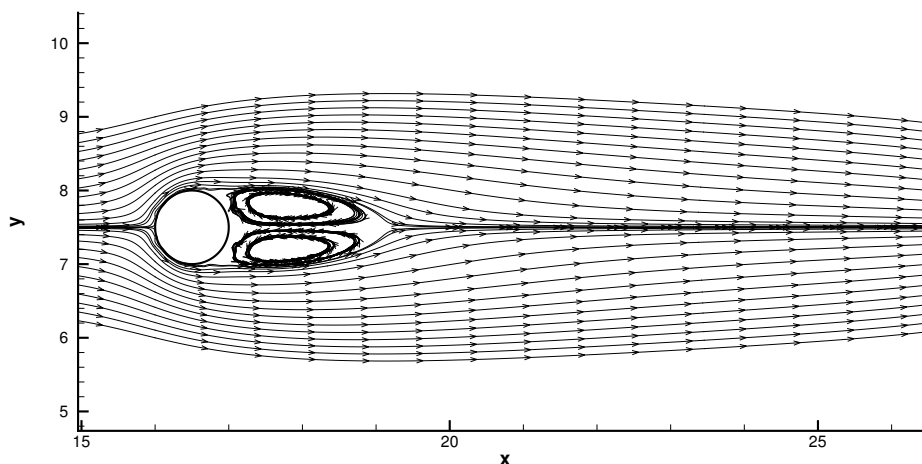


Figure 2. Streamlines results at $Re=30$.

Table 1. Comparison of the Wake Proprieties behind a Stationary Cylinder with Experiments and Previous Computational Results for $Re = 30$.

Proprieties of the wake	Present results	Saiki & Biringen	Coutanceau & Bouard	Clift et al.
Length of the separation bubble L_w	1.57	1.7	1.53	—
x-coordinate of the center of the VC	0.69	0.62	0.55	—
y-distance between the VC	0.62	0.5625	0.54	—
Separation angle	56.1°	48°	50.1°	—
Drag coefficient (C_d)	1.42	1.38	—	1.69

Table 2. Comparison of Strouhal number St from experiments and previous computational studies.

Reynolds number	Present results	Lima e Silva et al.	Roshko	Saiki & Biringen
100	0.145	0.16	0.167	0.171
150	0.162	0.18	—	—
300	0.172	0.20	0.19	—

Table 1 shows a comparison of the physical parameters of the separation bubble obtained with the present code with the computational study of Saiki and Biringen (1996), and experimental studies of Countanceau and Bouard (1977) and Clift et al (1978). In this table VC stands for Vortex Cores. A good agreement was obtained with this Reynolds number.

In Fig. 3 the streamlines are shown for $Re = 45$. It should be noted that for this Reynolds number the flow remains stable. Comparing this figure with Fig. 2 it can be observed that the length of the recirculation bubble increases with the Reynolds number. The recirculation bubble length obtained with this simulations was $L_w = 3.32$.

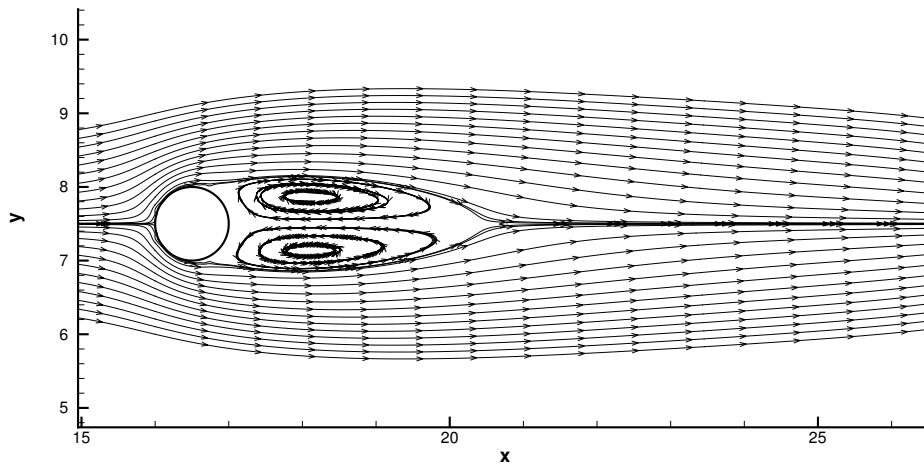


Figure 3. Streamlines results at $Re=45$.

Figures 4 to 6 show the vorticity field of simulations carried out with Reynolds numbers of 100, 150 and 300 respectively. It can be observed that the vorticity increases with Reynolds number, as expected. In these figures an oscillation in the front of the cylinder was achieved. These oscillations are attributed to the use of high order finite differences with immersed boundary technique (Saiki and Biringen, 1996).

The Strouhal number, defined as the dimensionless frequency with which the vortices are shed behind the body, was measured in these simulations and the results are shown in Tab. 2. In the same table are shown the results obtained by numerical simulations by Lima e Silva et al. (2003), Saiki and Biringen (1996) and experimental results (Roshko, 1955). It can be observed in this table that the Strouhal number obtained in the present simulations are smaller than the other results.

The variation of the drag coefficients with dimensionless time is shown in Fig.7. The results obtained for Reynolds number of 30, 45, 100, 150 and 300 are shown. The behavior of the unsteady flow simulations ($Re > 50$) starting with a lower value and increasing with time was also observed in the results of Lima e Silva et al. (2003). This can be explained as a result of the simulation start up.

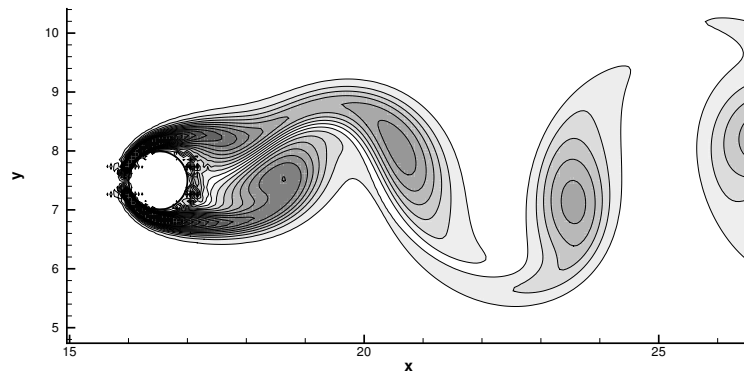


Figure 4. Vorticity contours at $Re=100$.

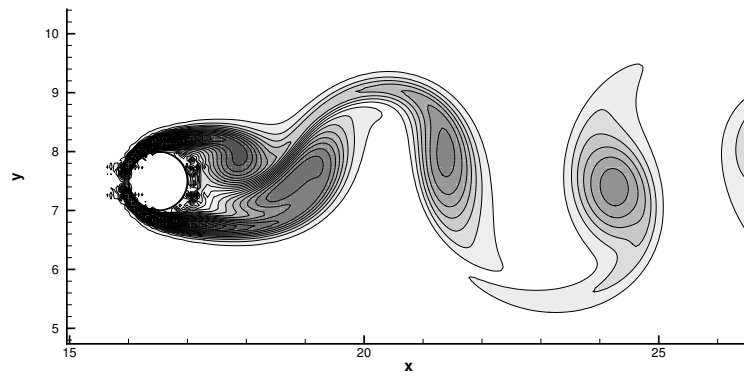


Figure 5. Vorticity contours at $Re=150$.

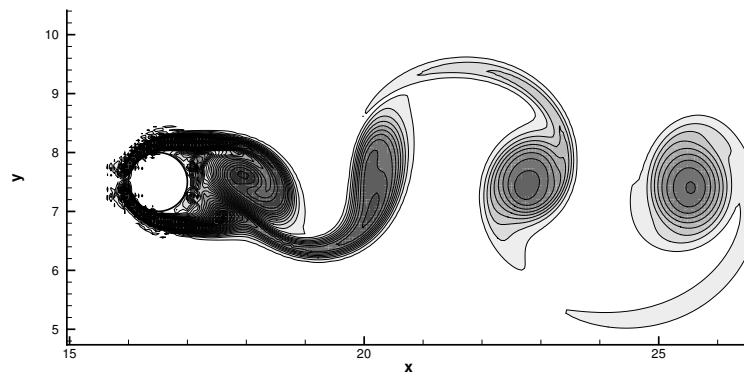


Figure 6. Vorticity contours at $Re=300$.

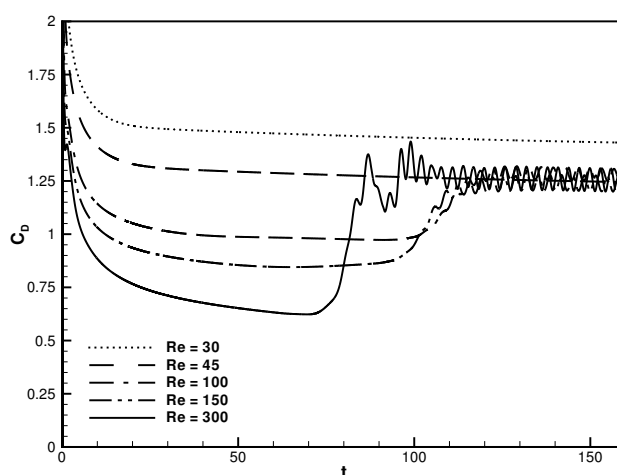


Figure 7. Variation of drag coefficients with dimensionless time, $Re = 30, 45, 100, 150$ and 300 .

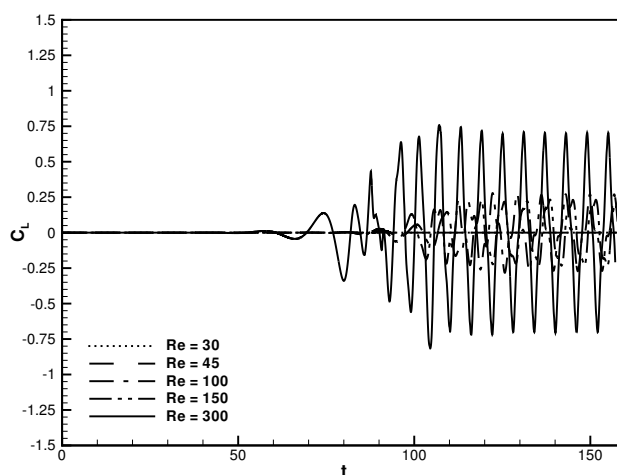


Figure 8. Variation of lift coefficients with dimensionless time, $Re = 30, 45, 100, 150$ and 300 .

Figure 8 shows the variation of lift coefficients with dimensionless time for Reynolds number of 30, 45, 100, 150 and 300. Here the oscillatory behavior of the lift coefficients for unsteady flow simulations ($Re > 50$) occurs after a certain simulation time.

5. Conclusions

In this paper, an immersed boundary technique was used to study steady/unsteady flows over a cylinder. The immersed boundary technique was used in a vorticity-velocity formulation. The computational results for both steady and unsteady flows compare favorably with both experiments and previous computational studies. Oscillations in front of the immersed body were achieved for Reynolds number greater than 100. These oscillations were attributed to the combination of high-order finite differences with immersed boundary technique. The use of filtering should damp these oscillations. The drag and lift coefficients are easily obtained with the immersed technique adopted. More investigations should be done with the present two-dimensional code before extending it to a three-dimensional code.

6. Acknowledgments

The author acknowledges the support received from FAPESP under grant No 04/07507-4.

7. References

- Balaras, E., (2003), Modeling Complex Boundaries Using an External Force Field on Fixed Cartesian Grids in Large-Eddy Simulations, "Computer & Fluids", Vol. .
- Clift, R., Grace, J. R., and Weber, M. E., (1978), "Bubbles, Drops and Particles", Academic Press, New York.

- Coutanceau, M. and Bouard, R., (1977), Experimental determination of the main features of the viscous flow in the wake of a circular cylinder in uniform translation. Part 1. Steady flow., "J. Fluid Mech.", Vol. **79**, pp. 231–256.
- Goldstein, D., Handler, R., and Sirovich, L., (1993), Modeling a No-Slip Flow Boundary with an External Force Field, "J. Computational Physics", Vol. **105**, pp. 354–366.
- Kloker, M., Konzelmann, U., and Fasel, H. F., (1993), Outflow Boundary Conditions for Spatial Navier-Stokes Simulations of Transition Boundary Layers, "AIAA Journal", Vol. **31**, pp. 620–628.
- Lai, M. and Peskin, C. S., (2000), An Immersed Boundary Method with Formal Second-Order Accuracy and Reduced Numerical Viscosity, "J. Comp. Phys.", Vol. 160, pp. 705–719.
- Lima e Silva, A. L. F., Silveira-Neto, A., and Damasceno, J. J. R., (2003), Numerical simulation of two-dimensional flows over a circular cylinder using the immersed boundary method, "J. Computational Physics", Vol. **189**, pp. 351–370.
- Linnick, M. N., (1999), Investigation of Actuators for use in Active Flow Control, Master's thesis, University of Arizona.
- Linnick, M. N. and Fasel, H., (2003), A High-Order Immersed Boundary Method for Unsteady Incompressible Flow Calculations, "41st Aerospace Sciences Meeting and Exhibit - AIAA-2003-1124".
- Meitz, H. L. and Fasel, H. F., (2000), A compact-difference scheme for the Navier-Stokes equations in vorticity-velocity formulation., "J. Comp. Phys.", Vol. **157**, pp. 371–403.
- Mohd-Yusof, J., (1997), Combined immersed-boundary/b-spline methods for simulation of flow in complex geometries, "Annual Research Briefs – Center for Turbulent Research", Vol. 1997, pp. 317–324.
- Mohd-Yusof, J., (1998), Development of Immersed Boundary Methods for Complex Geometries, "Annual Research Briefs – Center for Turbulent Research", Vol. 1998, pp. 325–336.
- Peskin, C. S., (1972), Flow Patterns Around Heart Valves: A Numerical Method, "J. Computational Physics", Vol. **10**, pp. 252–271.
- Peskin, C. S., (1977), Numerical Analysis of Blood Flow in the Heart, "J. Computational Physics", Vol. **25**, pp. 220–252.
- Roshko, A., (1955), On the wake and drag of bluff bodies, "J. Aeronaut. Sci.", Vol. **22**, pp. 124–132.
- Saiki, E. M. and Biringen, S., (1996), Numerical simulation of a cylinder in uniform flow: application of a virtual boundary method, "J. Comp. Phys.", Vol. **123**.
- Souza, L. F., Mendonça, M. T., de Medeiros, M. A. F., and Kloker, M., (2004), Seeding of Görtler Vortices Through a Suction and Blowing Strip, "RBCM - Journal of the Brazilian Society of Mechanical Sciences", Vol. XXVI, pp. 269–279.
- Souza, L. F., Mendonça, M. T., and Medeiros, M. A. F., (2005), The advantages of using high-order finite differences schemes in laminar-turbulent transition studies, "International Journal for Numerical Methods in Fluids", Vol. **48**, pp. 565–592.
- Stüben, K. and Trottenberg, U., (1981), "Nonlinear multigrid methods, the full approximation scheme", chapter 5, pp. 58–71, Lecture Notes in Mathematics. Köln-Porz.

8. Responsibility notice

The author(s) is (are) the only responsible for the printed material included in this paper